Journal of Biomechanics 71 (2018) 135–143

Contents lists available at ScienceDirect

Journal of Biomechanics

journal homepage: www.elsevier.com/locate/jbiomech
www.JBiomech.com

Estimation of unmeasured ground reaction force data based on the oscillatory characteristics of the center of mass during human walking

Hansol X. Ryu, Sukyung Park *

Department of Mechanical Engineering, Korea Advanced Institute of Science and Technology (KAIST), Daejeon, Republic of Korea

ARTICLE INFO

Article history:
Accepted 31 January 2018

Keywords:
Ground reaction force
Center of mass
Center of pressure
Compliant legged walking model
Human walking

ABSTRACT

To enhance the wearability of portable motion-monitoring devices, the size and number of sensors are minimized, but at the expense of quality and quantity of data collected. For example, owing to the size and weight of low-frequency force transducers, most currently available wearable gait measurement systems provide only limited, if any, elements of ground reaction force (GRF) data. To obtain the most GRF information possible with a minimal use of sensors, we propose a GRF estimation method based on biomechanical knowledge of human walking. This includes the dynamics of the center of mass (CoM) during steady human gait resembling the oscillatory behaviors of a mass-spring system. Available measurement data were incorporated into a spring-loaded inverted pendulum with translating pivot. The spring stiffness and simulation parameters were tuned to match, as accurately as possible, the available data and oscillatory characteristics of walking. Our results showed that the model simulation estimated reasonably well the unmeasured GRF. Using the vertical GRF and CoP profile for gait speeds ranging from 0.93 to 1.89 m/s, the anterior-posterior (A-P) GRF was estimated and resulted in an average correlation coefficient of R = 0.982 ± 0.009. Even when the ground contact timing and gait speed information were alone available, our method estimated GRFs resulting in R = 0.969 ± 0.022 for the A-P and R = 0.891 ± 0.101 for the vertical GRFs. This research demonstrates that the biomechanical knowledge of human walking, such as inherited oscillatory characteristics of the CoM, can be used to gain unmeasured information regarding human gait dynamics.

1. Introduction

Recent developments in micro-inertial sensors and wearable motion trace systems have moved gait analysis from a lab-based set up to daily life (Brigante et al., 2011; Mancini et al., 2011; O'Donovan et al., 2009; Roetenberg et al., 2009). However, the size and number of sensors are reduced to enhance the convenience of wearability of wearable motion monitoring devices, at the expense of the quality and quantity of the data collected. For example, most wearable gait monitoring systems collect gait kinematics such as gait speed, gait frequency, and number of steps (Chen et al., 2008; Greene et al., 2010; Moore et al., 2007; Rebula et al., 2013) based mostly on inertial measurement units (IMUs); however, the kinetic information found in the ground reaction forces (GRFs) remains unmeasured due to the limitations of force transducers, which are generally larger and heavier than those of micro-IMUs (Kim et al., 2014; Lind et al., 2009; Liu et al., 2012; Veltink et al., 2005). Specifically, the sensitivity, frequency response characteristics, and capacity of the force transducer unit, such as piezoresistive sensors and strain gauge load cells, correlate with the size of the sensing unit. As a result, the increased mass and volume, altered surface characteristics and stiffness of shoes containing force sensors result in changes in gait: the system could become non-wearable or hinder natural walking (Kong and De Heer, 2009; van den Noort et al., 2011). Most current film-type plantar pressure sensors measure vertical GRF only (Luo et al., 1998; Price et al., 2016; Putti et al., 2007; Shu et al., 2010), excluding essential kinetic information about forward propulsion, such as anterior-posterior (A-P) GRF.

Instead of directly measuring GRFs during walking, there have been studies that suggest a mathematical model to represent or predict GRFs during walking depending on factors such as walking speed, body weight, age or gender (Chao et al., 1983; Keller et al., 1996; Racic and Brownjohn, 2011; Racic et al., 2009). However, these studies typically generated normative GRF patterns for the given condition and did not fully take into account the variability of a particular subject or particular step. Others estimated unmeasured GRFs from measured plantar pressure patterns using

* Corresponding author at: Department of Mechanical Engineering, KAIST, 335 Gwahangno, Yuseong-gu, Daejeon 305-701, Republic of Korea.

E-mail address: sukyungp@kaist.ac.kr (S. Park).

https://doi.org/10.1016/j.jbiomech.2018.01.046
0021-9290/

numerical correlations obtained from a previously established database (Fong et al., 2008; Rouhani et al., 2010; Savelberg and De Lange, 1999; Sim et al., 2015). GRF estimators are trained to formulate a numerical relationship between plantar pressure measurement and a portion of the GRFs to be estimated, using previously measured GRF data sets at various walking speeds, frequencies, cadences, and subject body parameters. Reported A-P GRF estimation accuracies are approximately R = 0.928 (Fong et al., 2008) and R = 0.982 (Rouhani et al., 2010) at a steady, self-selected walking speed. To obtain a reliable estimation of the unmeasured GRFs, significant efforts and cost of data collection under various walking conditions are required. Moreover, the estimation of GRF from a pressure film might be sensitive to insole alignment, which is susceptible to alignment error from the relative movement inside shoes or different shoe shapes.

We suggest that by applying knowledge of mechanical characteristics of human gait, additional gait information, such as unmeasured GRFs, could be extracted from direct measurements using relatively simple systems such as wearable watch-type fitness devices or in-sole-type walking monitoring devices. Recent studies of gait mechanics have shown that each component of the GRF is dynamically coupled through spring-mass mechanics (Geyer et al., 2006; Jung and Park, 2014; Seyfarth et al., 2006). Specifically, the motion of the CoM and GRFs was well represented by the oscillation of a spring-mass system, and effective leg stiffness increased with gait speed for both young and elderly subjects (Holt et al., 2003; Hong et al., 2013). The natural frequency of the spring-mass mechanics of human walking was highly correlated with gait frequency (Lee et al., 2014). With the introduction of center of pressure (CoP) translation, the compliant legged walking model reproduced the GRF data reasonably well for various gait speeds (Hong et al., 2013; Jung and Park, 2014; Whittington and Thelen, 2009). Based on these observations, we propose an estimation method for unmeasured GRFs during steady gait from limited data, using a biomechanical model. We consider the effect of differing types of data availability. The estimated GRF was compared with experimental GRF data to validate the proposed estimation method.

2. Methods

To estimate unmeasured GRFs, the available measurement data were incorporated into a biomechanical walking model. We consider four cases of data collection with differing levels of data availability. The minimal data case assumes a sensor on each foot, which measures ground contact timing and gait speed but does not measure force. Conversely, the maximal data case assumes a situation with additional force sensors that measure the vertical GRF (vGRF) and CoP translation. Model parameters and initial conditions that best matched the available data set were identified so that GRFs could be estimated from the model simulation. The schematics of the GRF estimation are shown in Fig. 1. Details of the models, parameter selections, and simulation process follow.

2.1. The spring-mass walking model

The model consists of a mass and a spring that represent the CoM and effective lower-limb stiffness of a human. In this model, GRFs are represented by the spring resistance forces of the springy leg, which are calculated by multiplying the stiffness k and the length change of the springy leg, $\Delta l = l - l_0$, where l and l_0 are the current and initial leg lengths. The pivot point was translated to represent the CoP translation from heel to toe during stance phases (Jung and Park, 2014) because a model with a fixed pivot point overestimates the rotational motion of the leg during the stance phase (Geyer et al., 2006; Lipfert et al., 2012) and does not produce GRFs that quantitatively match human data. The equations of motion of the mass-spring model over a single (Eq. (1a)) and double (Eq. (1b)) support phase of the gait cycle are obtained as follows:

$$\begin{cases} m\ddot{z} = k(l-l_0)\sin\theta - mg = k\left(\sqrt{z^2+(x-x_{CoP})^2}-l_0\right)\sin\theta - mg \\ m\ddot{x} = k(l-l_0)\cos\theta = k\left(\sqrt{z^2+(x-x_{CoP})^2}-l_0\right)\cos\theta \end{cases} \tag{1a}$$

$$\begin{cases} m\ddot{z} = k\left(\sqrt{z^2+(x-x_{\mathrm{CoP1}})^2}-l_0\right)\sin\theta_1 + k\left(\sqrt{z^2+(x-x_{\mathrm{CoP2}})^2}-l_0\right)\sin\theta_2 - mg \\ m\ddot{x} = k\left(\sqrt{z^2+(x-x_{\mathrm{CoP1}})^2}-l_0\right)\cos\theta_1 + k\left(\sqrt{z^2+(x-x_{\mathrm{CoP2}})^2}-l_0\right)\cos\theta_2 \end{cases} \tag{1b}$$

where m is the mass located at CoM, x and z are the displacements of the CoM in A-P and vertical directions, and x_{CoP} is the forward movement of the pivot point (Fig. 1). Subscripts 1 and 2 indicate the leading and trailing legs, respectively. The position of the CoM could also be formulated using polar coordinates referenced at each ground contact point: θ and l represent the angle and length of springy legs. Gravitational acceleration is denoted as g.

There are four model parameters, m, l_0, k, and the x_{CoP} profile, and two initial vectors, which are position $\mathbf{x}_i = (x_i, z_i)$ and velocity $\dot{\mathbf{x}}_i = (\dot{x}_i, \dot{z}_i)$ of the CoM. To reduce the number of free parameters, available measurement data were used to set the body mass m and the leg length l_0. The initial leg length l_0 was approximated to be proportional to the subject's measured height h: $0.57 \cdot h$; this factor was obtained from anthropomorphic data (Park et al., 1999). When CoP data were available, the data were incorporated as the forward movement of the ground contact point of the springy-legged model. A Tukey window was used to guarantee continuity of the CoP profiles at each end of the stance phase. When the CoP measurement was not available, a mathematical approximation of the observed CoP profiles was used (Jung and Park, 2014).

To determine the initial conditions for model simulation, based on previous observations, we estimated unknown initial conditions depending on an averaged gait speed $\bar{v}$ (Adamczyk and Kuo, 2009; Kim and Park, 2011). For example, the forward speed of the CoM at the onset of the heel strike $\dot{x}_i$ was reported to be close to the average gait speed $\bar{v}$ such that $\dot{x}_i \approx \bar{v}$ (Adamczyk and Kuo, 2009), so we set the initial condition of the forward speed to be $\dot{x}_i = \bar{v}$ for the simulation. Similarly, the initial vertical speed $\dot{z}_i$ was approximated to be proportional to the average speed $\bar{v}$ based on previous reports (Adamczyk and Kuo, 2009; Kim and Park, 2011); however, we observed that $\dot{z}_i$ tends to vary from this initial estimation more than $\dot{x}_i$ does, so $\dot{z}_i$ was tuned within a range of -30 to 0% of the average gait speed. The initial position $\mathbf{x}_i$ of the CoM at the onset of simulation—in this case, the double support phase—could be determined by specifying the length of the trailing leg l_{2i} and the step length d_i. The only free model parameter k, the leg stiffness, was tuned to best match the data. The tuning boundaries were chosen based on the averages of current and previous data collections for various gait speeds, as mentioned in the method section. The bounds of the states were chosen to cover approximately two standard deviations (~95%) from the average values of previous observations. Depending on the availability and/or reliability of the data, the numbers and types of parameters to be predetermined and/or tuned could be chosen differently. Values of the model, simulation parameters and their tuning ranges are listed in Table 1. The step period is denoted as T.

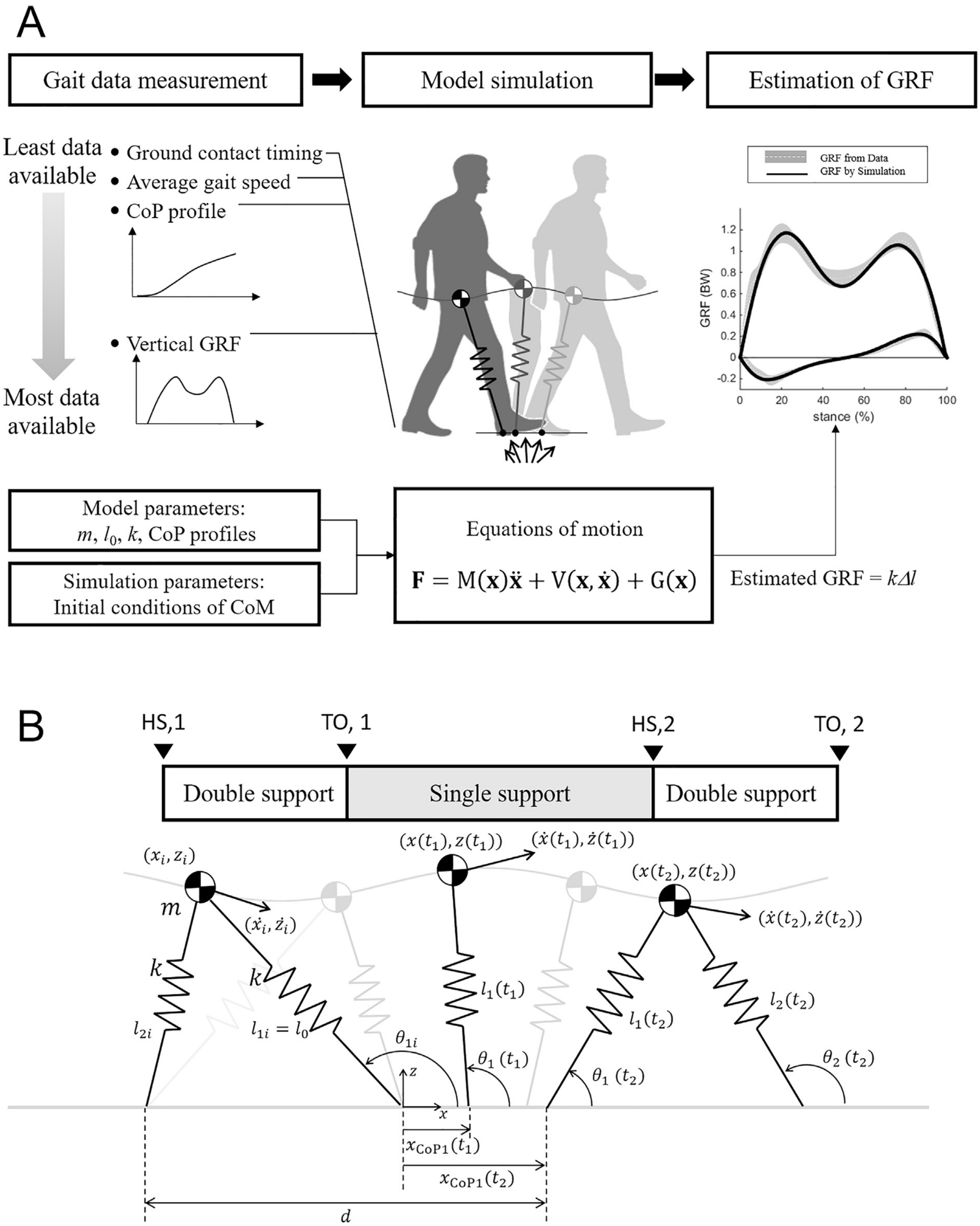

Fig. 1. (A) The process of unmeasured ground reaction force (GRF) estimation. The GRF was estimated from a model simulation of the compliant-legged walking model, which is known to describe the kinetics of the center of mass (CoM) well during human walking. The model parameter k, which is lower limb stiffness, and the simulation parameters of the initial conditions of the center of mass were tuned to best match the partially collected data available, such as ground contact timing, step length, and sometimes the vertical GRF. The pre-determined parameters were the subject's body mass and leg length. (B) Model details for each gait phase of the simulation. The position and the speed of the CoM in the forward and vertical directions in Cartesian coordinates referenced to the ground contact point of the stance foot are described as $\mathbf{x} = (x, z)$ and $\dot{\mathbf{x}} = (\dot{x}, \dot{z})$, respectively. The distance between the reference point and the CoP is represented as x_{CoP}. To describe the bipedal kinematics, the CoM motion was also described by leg length l and ground contact angle θ. Subscripts 1, 2, and i indicate the leading leg, the trailing leg, and the initial condition of the simulation, respectively. m, l_0, k, and d are the mass, the leg stiffness, the initial leg length, and the step length, respectively. Heel strike (HS) and toe off (TO) events of the leading leg and trailing leg are represented at the top. The amount of CoP excursion is exaggerated in the figure.

Table 1
Values and the tuning ranges for the model and simulation parameters.

Parameter notation	Description	Determination	Initial approximation	Tuning boundary
Model parameters				
m	Mass	Measured	–	–
l_0	Initial leg length	Measured	–	–
d_{foot}	Effective foot length	Measured	–	–
k	Effective leg stiffness	Tuned to match data	$k_0 = 40\frac{mg}{h}\bar{v}$	$(1 \pm 0.4)k_0$
Initial conditions				
d_i	Step length at the onset of double support	Tuned to match data	$d_0 = T \cdot \bar{v}$	$(1 \pm 0.15)d_0$
l_{2i}	Length of trailing at the onset of double support	Approximated	$l_{2i} \approx \frac{mg}{k}$	–
$\dot{x}_i$	Initial A-P velocity	Approximated	$\dot{x}_i \approx \bar{v}$	–
$\dot{z}_i$	Initial vertical velocity	Tuned to match data	$\dot{z}_{i0} = -0.15\bar{v}$	$(1 \pm 1)\dot{z}_{i0}$

2.2. Constraints and cost function of the model simulation

The springy walking model generates infinitely many solutions with various model parameters, so we could obtain multiple solutions that match the measured data reasonably well. Among those solutions, a solution that minimized an objective function was selected. We defined two objective functions depending on the available measurement data.

When vertical GRF data are available, an objective function was defined as the sum of the squared residual between the data and the model simulation (Eq. (2a)). The measured data and simulation were both discretized by 101 data points over one step.

When vertical GRF was not measured, we defined the objective function in an alternative way (Eq. (2b)). The residual between the data and the model simulation (Eq. (2a)) is unknown for this case. Instead, steady gait was assumed, and asymmetry between the left and right legs was penalized (Rummel et al., 2010). Specifically, the first term J_{height} penalizes vertical height differences between the first heel strike (HS) and second HS, and between the first toe off (TO) and second TO. GRF asymmetry within a single leg was not penalized because asymmetric GRF does not always mean an unstable gait (Merker et al., 2011). In addition, considering previous studies reporting CoM velocity during the step-to-step transition in human walking (Adamczyk and Kuo, 2009; Kim and Park, 2012), velocities deviating from the reported characteristics were also penalized. CoM velocity in the A-P direction at every HS and TO were all expected to be the same as the first HS, so differences were penalized ($J_{\text{vel\_x}}$). In a similar manner, CoM velocity in the vertical direction at HSs and TOs was expected to have the same amplitude, so differences were penalized ($J_{\text{vel\_z}}$). Since the cost function is composed of velocity and position terms, all terms were normalized by either the average walking speed or the leg length (Eq. (2b)):

$$\begin{aligned} \min J = \min J_{\text{GRF}} = \min \sum_{i=0}^{100} \left(\text{GRF}_{z,\text{data}}[i] - \text{GRF}_{z,\text{sim}}[i]\right)^2 \\ \text{where} \quad \text{GRF}\ [i] = \text{GRF}\left(t_{\text{HS},1} + (t_{\text{TO},2} - t_{\text{HS},1})\frac{i}{100}\right) \end{aligned} \tag{2a}$$

$$\begin{aligned} \min J &= \min\left[J_{\text{height}} + J_{\text{vel\_x}} + J_{\text{vel\_z}}\right] \\ &= \min\left[\frac{(z_{\text{HS},2} - z_{\text{HS},1})^2 + (z_{\text{TO},2} - z_{\text{TO},1})^2}{l_0^{\,2}}\right. \\ &\quad + \frac{(\dot{x}_{\text{HS},2} - \dot{x}_{\text{HS},1})^2 + (\dot{x}_{\text{TO},1} - \dot{x}_{\text{HS},1})^2 + (\dot{x}_{\text{TO},2} - \dot{x}_{\text{HS},1})^2}{\bar{v}^2} \\ &\quad \left. + \frac{(\dot{z}_{\text{HS},2} - \dot{z}_{\text{HS},1})^2 + (-\dot{z}_{\text{TO},1} - \dot{z}_{\text{HS},1})^2 + (-\dot{z}_{\text{TO},2} - \dot{z}_{\text{HS},1})^2}{\bar{v}^2}\right] \end{aligned} \tag{2b}$$

where $\text{GRF}_{z,data}$ and $\text{GRF}_{z,sim}$ are the vertical GRF profiles obtained from data and the simulation, respectively. The feasibility constraint that the force should be non-negative was applied to the GRF. To expedite the estimation process for the data of each step, and because each step does not show perfect steady-state periodicity of the gait parameters, we performed the estimation without restricting the results to a subset of limit cycles.

2.3. Data collection

Eight healthy young male subjects (22.0 ± 2.5 yr) participated in the study. They had an average weight of 66.9 ± 7.5 kg and a height of 172.9 ± 5.1 cm. Prior to data collection, subjects submitted an informed consent form that was approved by the IRB at KAIST.

Subjects walked on a force-plate instrumented custom-made treadmill for 1 min at four different randomly ordered gait speeds ranging from approximately 0.9 to 1.9 m/s. The self-selected walking speed (WS_{SS}) and maximum walking speed (WS_{MAX}) were measured over-ground, and the difference between the two walking speeds, represented as $\Delta WS = WS_{MAX} - WS_{SS}$, was obtained for each subject to determine the trial speeds. We performed tests at 4 walking speeds: $WS_{SS} - 0.25\Delta WS$, WS_{SS}, $WS_{SS} + 0.25\Delta WS$ and $WS_{SS} + 0.50\Delta WS$. Once the subjects reached a steady gait after approximately 30 s of walking, ten consecutive steps were used for data analysis.

GRFs under each foot were measured from the force plate (Bertec, US) at a sampling rate of 800 Hz and were filtered using a Butterworth fifth-order low-pass filter with a cut-off frequency of 20 Hz to eliminate high-frequency noise without significant distortion of the data. The CoP trajectories were calculated from the force plate data, which was low-pass filtered with a cut-off frequency of 10 Hz to suppress the high-frequency noise of the CoP velocity and acceleration, which were used for the simulation. The stance phase duration was defined using the vertical ground reaction force data. The GRF data showed impulsive disturbances right after HS but showed prolonged non-zero but negligible contact force near TO, so the stance phase was defined by the periods where the vertical GRF was greater than 40 N. Estimated GRFs were compared with measured GRFs from the force plate. The correlation coefficient R and normalized root-mean-square error (NRMSE), defined as the root-mean-square error divided by the range of the measured data, were calculated.

3. Results

The proposed GRF estimation method demonstrated a reasonably good match between the data and the estimation (Figs. 2 and 3, Table 2). It was tested for a total of 320 trials of 8 subjects at four different gait speeds ranging from 0.93 m/s to 1.89 m/s. The proposed estimation method produced feasible simulation results for 317 trials out of 320 trials (99.1%). Fig. 4 shows the tune leg stiffness k as a function of walking speed. Consistent with the

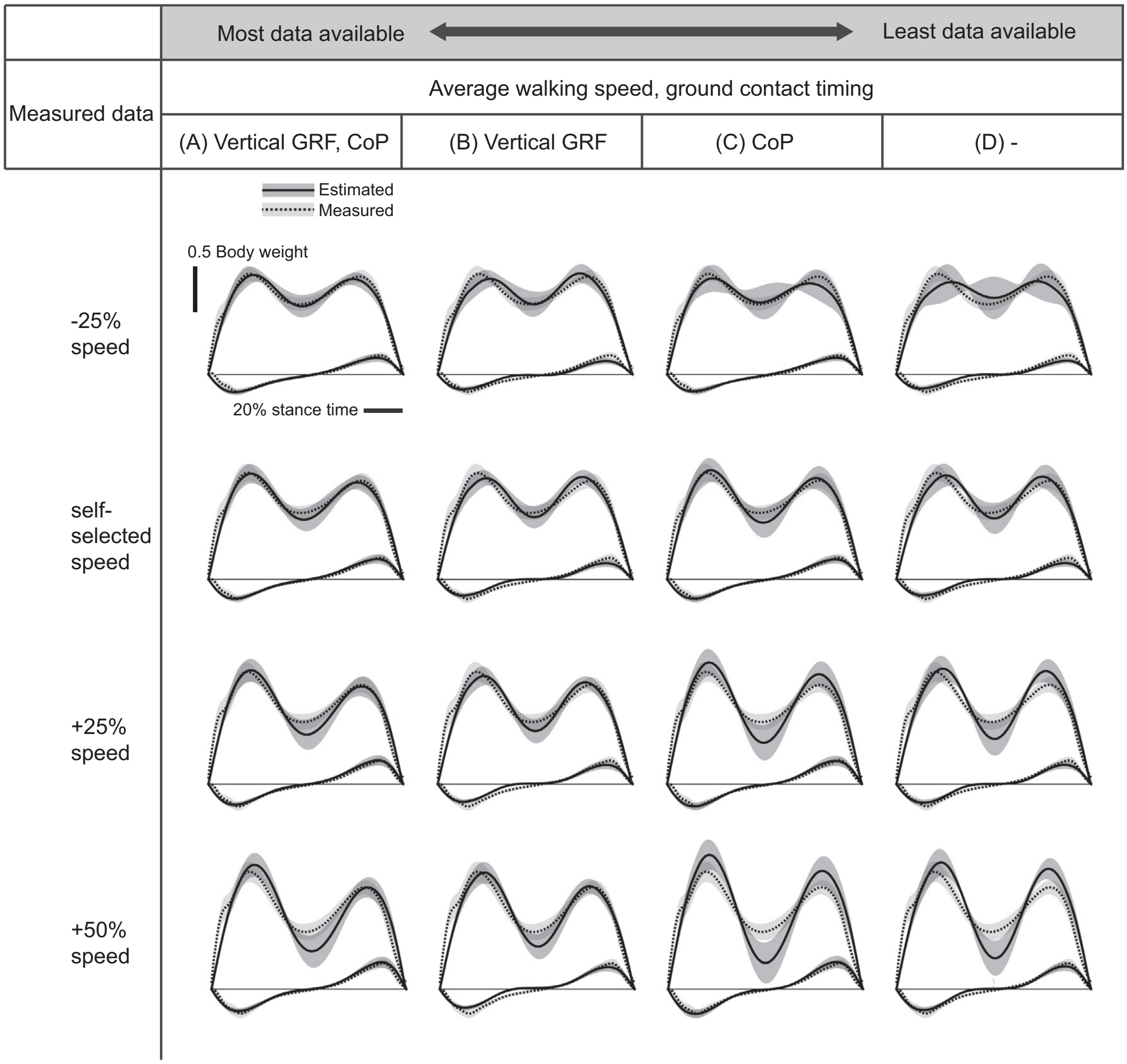

Fig. 2. Estimated (solid line) GRFs and measured (dashed line) GRFs with one standard deviation (shaded areas) at each gait speed for 8 subjects with the (A) most to (D) least data availability. Specifically, the estimation was performed when the available measurement data were average walking speed, ground contact timing, in addition to (A) the vertical GRF and CoP, (B) only the vertical GRF, (C) only the CoP, and (D) neither vertical GRF nor CoP.

existing literature (Kim and Park, 2011), stiffness k increases with speed regardless of the availability of the measured data.

When the model estimation was incorporated with the measured CoP profiles to match the measured vertical GRF, the average normalized NRMSE of the A-P GRF estimation from the 320 trials at four different gait speeds was 7.03 ± 1.78% with an average correlation coefficient of R = 0.982 ± 0.009 (Figs. 2 and 3, Table 2). In this case, vertical GRFs were reproduced from the simulation with an NRMSE of 8.98 ± 3.82% and R = 0.941 ± 0.038. When only ground contact time and average walking speed information was available, the average NRMSE of the A-P and vertical GRF estimations increased to 8.25 ± 2.40% and 12.51 ± 4.73% (Figs. 2 and 3, Table 2), with average correlation coefficients of R = 0.969 ± 0.022 and 0.891 ± 0.101, respectively. The performance of the A-P GRF estimation improved significantly ($p < 0.0001$) with the availability of CoP profile data, while the vertical GRF estimation results did not improve significantly ($p = 0.064$). Conversely, the availability of vertical GRF data did not improve the performance of the A-P GRF estimation significantly ($p = 0.093$) (Fig. 3, Table 2). The compliant-legged walking model could estimate the unmeasured vertical GRF around the slow-to-mid range of the gait speed well, while it estimated the A-P GRF better at the mid-to-high range of gait speed (Fig. 3, Table 2).

4. Discussion

Our study examined whether knowledge of human gait dynamics based on spring mechanics could enhance the quality and/or quantity of the partially measured gait data. Using the oscillatory characteristics of gait dynamics, unmeasured GRFs were successfully reconstructed from limited gait information, though the degree of agreement between the data and the estimation depends on the availability of the measured gait parameters and the gait speed. Whereas springy mechanics contribute to the qualitative characteristics of the GRF profiles, the CoP movement emulated by the translating ground contact point enhances the quantitative match between the model and data (Figs. 2 and 3, Table 2), as reported in previous studies (Jung and Park, 2014; Kim and Park, 2011; Whittington and Thelen, 2009).

The A-P GRF estimation results from previous studies have ranges that are larger than or similar to those of the current study, with more data used to train an estimator. A previous study

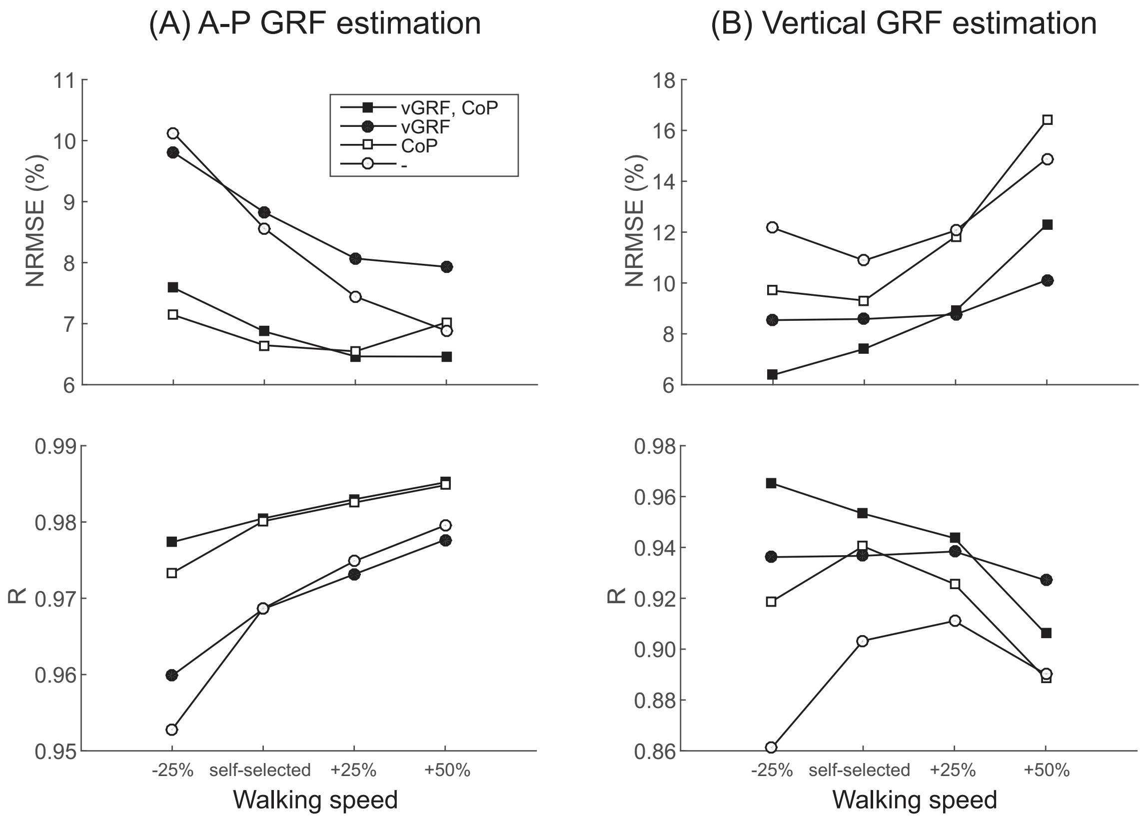

Fig. 3. The average NRMSE and R of the (A) A-P GRF and (B) vertical GRF estimations at four different gait speeds with four cases of data availability.

Table 2
Simulation results depending on the data availability, for the (A) 25% slower, (B) self-selected, (C) 25% faster, and (D) 50% faster walking speed. The results are expressed as the average ± one standard deviation.

Available measurement in addition to average walking speed, ground contact timing	A-P GRF estimation		Vertical GRF fitting/estimation	
	NRMSE (%)	R	NRMSE (%)	R
(A) 25% slower walking speed				
vGRF and CoP	7.59 ± 1.71	0.977 ± 0.009	6.38 ± 1.71	0.965 ± 0.021
vGRF	9.81 ± 2.24	0.960 ± 0.018	8.54 ± 3.03	0.936 ± 0.075
CoP	7.14 ± 1.76	0.973 ± 0.015	9.70 ± 3.82	0.919 ± 0.080
–	10.13 ± 2.52	0.953 ± 0.028	12.16 ± 6.53	0.861 ± 0.171
(B) self-selected walking speed				
vGRF and CoP	6.87 ± 1.69	0.980 ± 0.008	7.41 ± 2.49	0.953 ± 0.031
vGRF	8.82 ± 1.80	0.969 ± 0.016	8.58 ± 1.99	0.937 ± 0.035
CoP	6.65 ± 1.70	0.980 ± 0.009	9.31 ± 3.17	0.940 ± 0.029
–	8.56 ± 2.19	0.969 ± 0.022	10.89 ± 3.38	0.903 ± 0.079
(C) 25% faster walking speed				
vGRF and CoP	6.46 ± 1.60	0.983 ± 0.008	8.90 ± 3.16	0.944 ± 0.030
vGRF	8.07 ± 1.59	0.973 ± 0.013	8.76 ± 2.00	0.938 ± 0.029
CoP	6.55 ± 1.87	0.983 ± 0.009	11.82 ± 3.83	0.926 ± 0.027
–	7.44 ± 1.95	0.975 ± 0.014	12.06 ± 3.48	0.911 ± 0.041
(D) 50% faster walking speed				
vGRF and CoP	6.46 ± 1.64	0.985 ± 0.007	12.30 ± 3.79	0.906 ± 0.041
vGRF	7.93 ± 1.44	0.978 ± 0.010	10.11 ± 2.85	0.927 ± 0.039
CoP	7.02 ± 2.46	0.985 ± 0.007	16.41 ± 5.28	0.889 ± 0.048
–	6.89 ± 1.46	0.980 ± 0.011	14.89 ± 3.93	0.890 ± 0.050

reported an NRMSE of 12% and a correlation coefficient R = 0.928 for A-P GRF estimation when validated with subjects who were not included in their database (Fong et al., 2008). Another study reported an NRMSE of 7.2% and R = 0.982 (Rouhani et al., 2010) for intra-subject trainings, which use a subject-specific database. It was also reported that with an inter-subject training strategy, the NRMSEs increased approximately twofold (Rouhani et al., 2010) compared to intra-subject training, suggesting that many walking trials from various subjects at various gait speeds are needed to guarantee high reliability for these methods.

The simple springy model, nevertheless, showed limitations in reconstructing the GRF data owing to its simplicity. First, the

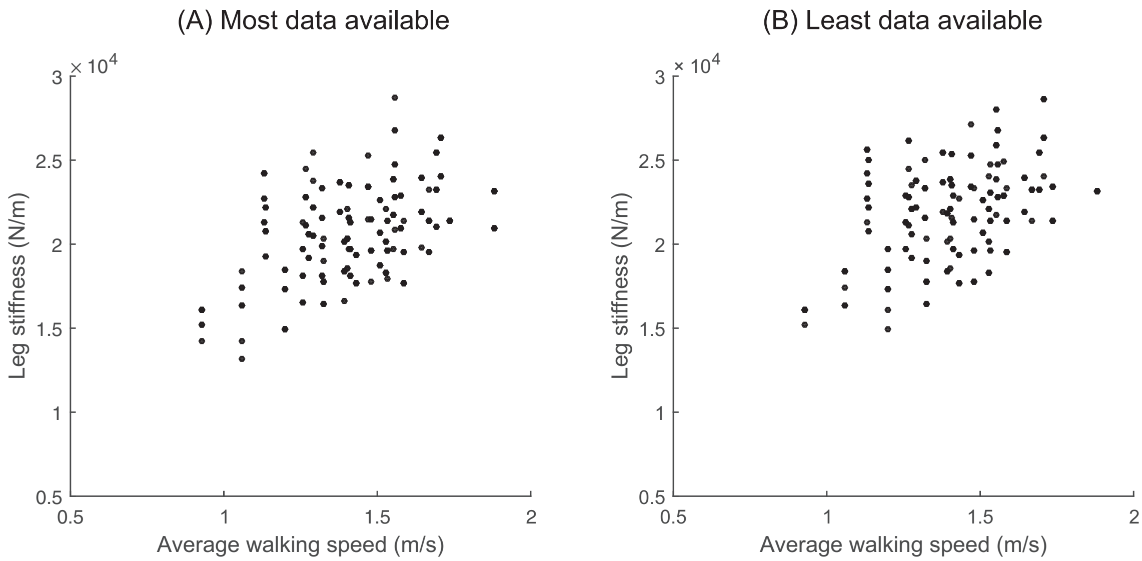

Fig. 4. The values of tuned leg stiffness k that results in the best match between data and simulation when the (A) most data and (B) least data were available. The results of the model simulation with tuned stiffness k are used for estimation of unmeasured GRF.

spring-mass walking model with a massless foot is not capable of representing the high-frequency component of walking, which is especially observable during heel strike. When a massed foot hits the ground during human gait, an impulsive force that induces a momentum change in the massed foot is applied to the ground, which is reflected as the impact peak. However, with continuous compression of the spring under a perfect elastic collision assumption, the spring-mass model could not reproduce the impact transient, which is a local bump in the ground reaction force occurring near heel strike (Fig. 2).

Another source of estimation errors is the inaccuracy of the CoP translation profile. A previous study showed that the acceleration of CoP could be well approximated by a continuous single sinusoid of the resonant frequency of the spring-mass system (Jung and Park, 2014). However, our data showed that 3 of the 8 subjects' CoP had large differences compared to the sinusoidal approximation (Fig. 5). The different CoP velocity profiles observed among test subjects indicates that gait patterns may vary significantly even among a homogeneous subject group. Despite this difference, the GRFs of those subjects could still be reproduced with the compliant legged walking model; the addition of CoP measurement significantly improved the estimation results (Fig. 5). This result implies the importance of accounting for CoP translation in walking dynamics modeling, as was reported in a previous study (Jung and Park, 2014).

As we are interested in estimating an unmeasured quantity from known information rather than in obtaining model parameters that give solutions, a large solution domain helps us to easily approximate the unmeasured quantity from the model. Model parameters may vary among those solutions: for example, the leg stiffness k showed strong correlation with gait speed in previous studies (Kim and Park, 2011), but the tuned stiffness k from our study showed weak proportionality with speed (Fig. 4). We observed that the speed proportionality of leg stiffness is abated when other variables such as the step length and vertical speed at the onset of double support are also simulated as tuning variables. However, although tuning parameters may vary due to the large solution domain, high correlations between GRFs and measurements still hold in the solution domain, allowing us to obtain reliable GRF estimates. It is worth noting that one may select or tune the model and/or simulation parameters differently depending on the reliability of the measurement data and the allowable computational cost.

Several wearable motion-monitoring devices based on inertial measurement units (IMU) are currently available; these systems provide mostly kinematic information. On the other hand, miniaturized force or pressure sensors embedded in a shoe have been used to measure partial components of the vertical GRF (Kim et al., 2014) or plantar pressure (Fong et al., 2008; Price et al., 2016; Putti et al., 2007), but they provide only limited kinetics information. By incorporating these systems into the proposed GRF estimation method, the quantity and quality of the output data could be enhanced. Additional gait information would be helpful for several applications, such as gait normality monitoring, gait rehabilitation progress assessment, and daily exercise tracking. For example, the asymmetries of estimated GRFs between each leg could be monitored during steady gait of patients with arthritis or anterior cruciate ligament tear. Additional gait dynamics information such as mechanical work done, efficiency of forward propulsion calculated from A-P GRF, or magnitude of heel strike impact would improve user experience when monitoring daily walking exercise using wearable devices.

The proposed estimation method is based on the premise that there is a resemblance between the walking dynamics and springy mechanics. These observations, however, are based on the steady gait data of healthy young (Lee et al., 2014) and elderly subjects (Hong et al., 2013). The application of the current method to estimate the transient gait data and/or gait of an individual patient is limited, and further study of the mechanics of these non-steady gaits or patients' gaits should be conducted. Examining GRFs of perturbed gait using the proposed method to identify the affected gait dynamics would enhance its value if the measured data were similar to springy mechanics. In addition, the accuracy of the estimation depends on both the accuracy of the available data and the resemblance of the gait dynamics to springy mechanics. When the proposed method is applied to portable gait-monitoring devices, which currently are less accurate than non-portable equipment such as force plates, the performance of GRF estimation would be lower than what is reported in this study. The amount of accuracy of GRF estimation that is helpful for recognizing gait normality or the progress of gait rehabilitation should be examined further.

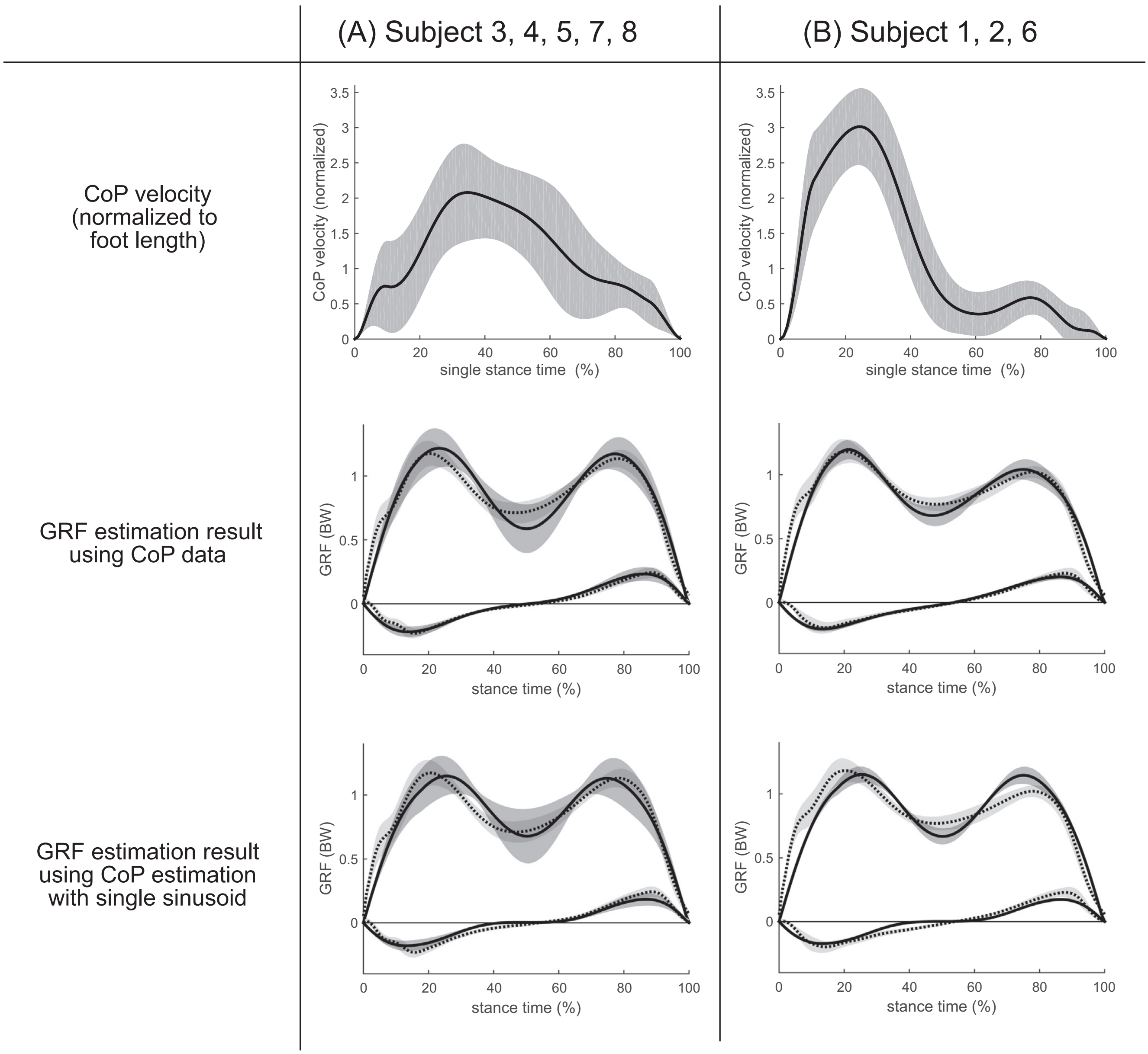

Fig. 5. Two types of CoP speed profiles (first row) and the corresponding GRF estimation results from the model incorporating the CoP data (middle row) and the CoP estimation (bottom row). Empirical data showed two distinct CoP speed profiles with the peak CoP speed occurring around (A) the mid- and (B) early-stance phase. Five and three subjects of all 8 participants showed peak CoP during the mid- and early-stance phases, respectively.

Conflicts of interest

None.

Acknowledgments

This work was supported by the National Research Foundation of Korea (NRF) grant funded by the Korea government (MSIT) (No. 2016R1A2B4007224).

References

Adamczyk, P.G., Kuo, A.D., 2009. Redirection of center-of-mass velocity during the step-to-step transition of human walking. J. Exp. Biol. 212, 2668–2678.

Brigante, C.M., Abbate, N., Basile, A., Faulisi, A.C., Sessa, S., 2011. Towards miniaturization of a MEMS-based wearable motion capture system. IEEE Trans. Ind. Electron. 58, 3234–3241.

Chao, E.Y., Laughman, R.K., Schneider, E., Stauffer, R.N., 1983. Normative data of knee joint motion and ground reaction forces in adult level walking. J. Biomech. 16, 219–233.

Chen, M., Huang, B., Xu, Y., 2008. Intelligent shoes for abnormal gait detection. In: Robotics and Automation, 2008. ICRA 2008. IEEE International Conference on.

Fong, D.T., Chan, Y.Y., Hong, Y., Yung, P.S., Fung, K.Y., Chan, K.M., 2008. Estimating the complete ground reaction forces with pressure insoles in walking. J. Biomech. 41, 2597–2601.

Geyer, H., Seyfarth, A., Blickhan, R., 2006. Compliant leg behaviour explains basic dynamics of walking and running. Proc. Biol. Sci. 273, 2861–2867.

Greene, B.R., McGrath, D., O'Neill, R., O'Donovan, K.J., Burns, A., Caulfield, B., 2010. An adaptive gyroscope-based algorithm for temporal gait analysis. Med. Biol. Eng. Comput. 48, 1251–1260.

Holt, K.G., Wagenaar, R.C., LaFiandra, M.E., Kubo, M., Obusek, J.P., 2003. Increased musculoskeletal stiffness during load carriage at increasing walking speeds maintains constant vertical excursion of the body center of mass. J. Biomech. 36, 465–471.

Hong, H., Kim, S., Kim, C., Lee, S., Park, S., 2013. Spring-like gait mechanics observed during walking in both young and older adults. J. Biomech. 46, 77–82.

Jung, C.K., Park, S., 2014. Compliant bipedal model with the center of pressure excursion associated with oscillatory behavior of the center of mass reproduces the human gait dynamics. J. Biomech. 47, 223–229.

Keller, T., Weisberger, A., Ray, J., Hasan, S., Shiavi, R., Spengler, D., 1996. Relationship between vertical ground reaction force and speed during walking, slow jogging, and running. Clin. Biomech. 11, 253–259.

Kim, J.-C., Kim, K.-S., Kim, S., 2014. Wearable sensor system including optical 3-axis GRF sensor for joint torque estimation in real-time gait analysis. In: 2014 IEEE/ASME International Conference on Advanced Intelligent Mechatronics.

Kim, S., Park, S., 2011. Leg stiffness increases with speed to modulate gait frequency and propulsion energy. J. Biomech. 44, 1253–1258.

Kim, S., Park, S., 2012. The oscillatory behavior of the CoM facilitates mechanical energy balance between push-off and heel strike. J. Biomech. 45, 326–333.

Kong, P.W., De Heer, H., 2009. Wearing the F-Scan mobile in-shoe pressure measurement system alters gait characteristics during running. Gait Posture 29, 143–145.

Lee, M., Kim, S., Park, S., 2014. Resonance-based oscillations could describe human gait mechanics under various loading conditions. J. Biomech. 47, 319–322.

Lind, R.F., Love, L.J., Rowe, J.C., Pin, F.G., 2009. Multi-axis foot reaction force/torque sensor for biomedical applications. In: 2009 IEEE/RSJ International Conference on Intelligent Robots and Systems.

Lipfert, S.W., Gunther, M., Renjewski, D., Grimmer, S., Seyfarth, A., 2012. A model-experiment comparison of system dynamics for human walking and running. J. Theor. Biol. 292, 11–17.

Liu, T., Inoue, Y., Shibata, K., Shiojima, K., 2012. A mobile force plate and three-dimensional motion analysis system for three-dimensional gait assessment. IEEE Sens. J. 12, 1461–1467.

Luo, Z.P., Berglund, L.J., An, K.N., 1998. Validation of F-Scan pressure sensor system: a technical note. J. Rehabil. Res. Dev. 35, 186–191.

Mancini, M., King, L., Salarian, A., Holmstrom, L., McNames, J., Horak, F.B., 2011. Mobility lab to assess balance and gait with synchronized body-worn sensors. J. Bioeng. Biomed. Sci. Suppl. 1, 007.

Merker, A., Rummel, J., Seyfarth, A., 2011. Stable walking with asymmetric legs. Bioinspir. Biomim. 6, 045004.

Moore, S.T., MacDougall, H.G., Gracies, J.M., Cohen, H.S., Ondo, W.G., 2007. Long-term monitoring of gait in Parkinson's disease. Gait Posture 26, 200–207.

O'Donovan, K.J., Greene, B.R., McGrath, D., O'Neill, R., Burns, A., Caulfield, B., 2009. SHIMMER: A new tool for temporal gait analysis. In: 2009 Annual International Conference of the IEEE Engineering in Medicine and Biology Society.

Park, S.J., Park, S.C., Kim, J.H., Kim, C.-B., 1999. Biomechanical parameters on body segments of Korean adults. Int. J. Ind. Ergon. 23, 23–31.

Price, C., Parker, D., Nester, C., 2016. Validity and repeatability of three in-shoe pressure measurement systems. Gait Posture 46, 69–74.

Putti, A.B., Arnold, G.P., Cochrane, L., Abboud, R.J., 2007. The Pedar in-shoe system: repeatability and normal pressure values. Gait Posture 25, 401–405.

Racic, V., Brownjohn, J.M.W., 2011. Stochastic model of near-periodic vertical loads due to humans walking. Adv. Eng. Inf. 25, 259–275.

Racic, V., Pavic, A., Brownjohn, J., 2009. Experimental identification and analytical modelling of human walking forces: Literature review. J. Sound Vib. 326, 1–49.

Rebula, J.R., Ojeda, L.V., Adamczyk, P.G., Kuo, A.D., 2013. Measurement of foot placement and its variability with inertial sensors. Gait Posture 38, 974–980.

Roetenberg, D., Luinge, H., Slycke, P., 2009. Xsens MVN: full 6DOF human motion tracking using miniature inertial sensors. Xsens Motion Technologies BV, Tech. Rep.

Rouhani, H., Favre, J., Crevoisier, X., Aminian, K., 2010. Ambulatory assessment of 3D ground reaction force using plantar pressure distribution. Gait Posture 32, 311–316.

Rummel, J., Blum, Y., Maus, H.M., Rode, C., Seyfarth, A., 2010. Stable and robust walking with compliant legs. In: Robotics and automation (ICRA), 2010 IEEE international conference on.

Savelberg, H., De Lange, A., 1999. Assessment of the horizontal, fore-aft component of the ground reaction force from insole pressure patterns by using artificial neural networks. Clin. Biomech. 14, 585–592.

Seyfarth, A., Geyer, H., Blickhan, R., Lipfert, S., Rummel, J., Minekawa, Y., Iida, F., 2006. Running and Walking with Compliant Legs, Fast Motions in Biomechanics and Robotics. Springer, pp. 383–401.

Shu, L., Hua, T., Wang, Y., Qiao Li, Q., Feng, D.D., Tao, X., 2010. In-shoe plantar pressure measurement and analysis system based on fabric pressure sensing array. IEEE Trans. Inf. Technol. Biomed. 14, 767–775.

Sim, T., Kwon, H., Oh, S.E., Joo, S.B., Choi, A., Heo, H.M., Kim, K., Mun, J.H., 2015. Predicting complete ground reaction forces and moments during gait with insole plantar pressure information using a wavelet neural network. J. Biomech. Eng. 137.

van den Noort, J., van der Esch, M., Steultjens, M.P., Dekker, J., Schepers, M., Veltink, P.H., Harlaar, J., 2011. Influence of the instrumented force shoe on gait pattern in patients with osteoarthritis of the knee. Med. Biol. Eng. Compu. 49, 1381–1392.

Veltink, P.H., Liedtke, C., Droog, E., van der Kooij, H., 2005. Ambulatory measurement of ground reaction forces. IEEE Trans. Neural Syst. Rehabil. Eng. 13, 423–427.

Whittington, B.R., Thelen, D.G., 2009. A simple mass-spring model with roller feet can induce the ground reactions observed in human walking. J. Biomech. Eng. 131, 011013.